IEEE Photonics Journal
An IEEE Photonics Society Publication

Open Access

Enhancing the Performance of Blue Quantum-Dot Light-Emitting Diodes Based on Mg-Doped ZnO as an Electron Transport Layer

Volume 9, Number 2, April 2017

Min-Ming Yan
Yi Li
Yong-Tian Zhou
Li Liu
Yong Zhang
Bao-Gui You
Yang Li

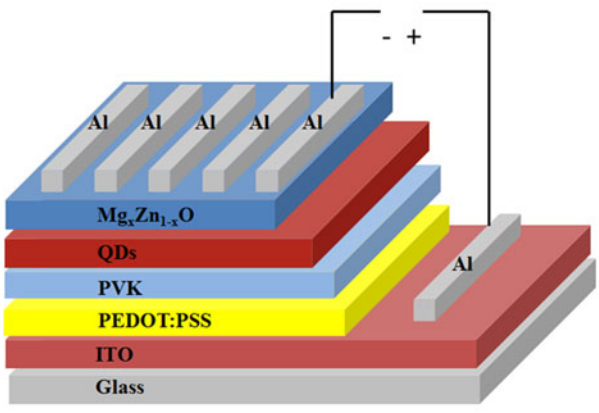

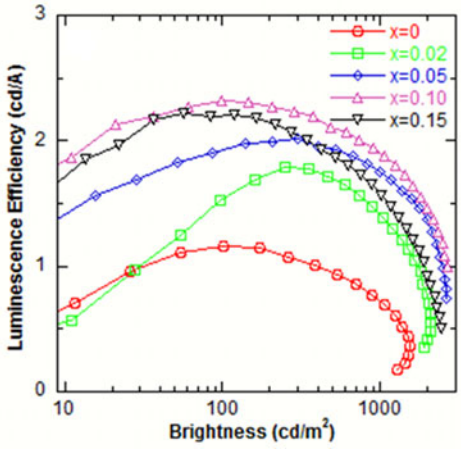

DOI: 10.1109/JPHOT.2017.2666423
1943-0655 © 2017 IEEE

Enhancing the Performance of Blue Quantum-Dot Light-Emitting Diodes Based on Mg-Doped ZnO as an Electron Transport Layer

Min-Ming Yan,[1] Yi Li,[1] Yong-Tian Zhou,[1] Li Liu,[1] Yong Zhang,[1,2] Bao-Gui You,[3] and Yang Li[3]

[1]Laboratory of Nanophotonic Functional Materials and Devices, Institute of Optoelectronic Materials and Technology, South China Normal University, Guangzhou 510631, China
[2]Guangdong Engineering Technology Research Center of Low Carbon and Advanced Energy Materials, Guangzhou 510631, China
[3]Guangdong Poly Optoelectronic Co., Ltd., Jiangmen 529020, China

DOI:10.1109/JPHOT.2017.2666423

Manuscript received January 30, 2017; revised February 3, 2017; accepted February 6, 2017. Date of publication March 7, 2017; date of current version March 23, 2017. This work was supported in part by the Nature Science Foundation of China under Grant 61377065 and Grant 61574064, in part by the Science and Technology Planning Project of Guangdong Province under Grant 2013CB040402009 and Grant 2015B010132009, and in part by the Science and Technology Project of Guangzhou City under Grant 2014J4100056. Corresponding author: Y. Zhang (e-mail: zycq@scnu.edu.cn).

Abstract: Highly efficient blue quantum-dot light-emitting diodes (QD-LEDs) have been fabricated by substituting Mg-doped ZnO ($Mg_xZn_{1-x}O$) for ZnO as an electron transporting layer (ETL). The device performance can be enhanced by optimizing Mg-doped ratios for the device structure of ITO/PEDOT:PSS/PVK/QDs/$Mg_xZn_{1-x}O$/Al. The maximum luminescence efficiency and maximum brightness of blue QD-LEDs increase from 1.1 cd/A and 1500 cd/m^2 for ZnO to 2.3 cd/A and 2500 cd/m^2 for 10% Mg-doped ZnO ($Mg_{0.10}Zn_{0.90}O$), respectively. The improved device performance should be attributed to balance electron and hole injection due to Mg-doped ZnO increasing the band gap and reduce exciton loss at the interface between the ETL and the emissive layer.

Index Terms: Light-emitting diodes (LEDs), quantum dots (QDs), ZnO, Mg-doped ZnO, electron transporting layers (ETLs).

1. Introduction

Colloidal quantum dot (QD) is a novel optoelectronic material and has recently been widely investigated for its application in biological imaging [1], [2], photodetectors [3], [4], solar cells [5], [6], and light-emitting diodes (LEDs) [7], [8]. Using QDs as an emitting layer is as known as quantum-dot light-emitting diodes (QD-LEDs), which are considered as next-generation light-emitting diodes that can be potentially used in the display technology [9] due to its pure and saturated color emission with a narrow bandwidth, tunable colors, high luminescence quantum yield, and simple fabrication process [10]–[15]. However, for QD-LEDs, the devices based on small molecules as electron transporting layer (ETL) such as Alq_3 [16] and TPBi [17] have inferior thermal stability and are more susceptible to degradation induced by oxygen and moisture. Therefore, using metal oxides like ZnO and TiO_2 as a substitute for organic material counterparts has been proposed [18]–[20]. Even

though using ZnO as ETL can enhance the performance of devices, the unbalanced hole and electron injection is still a primary problem to limit the performance of the device because the electron mobility of ZnO is generally higher than the hole mobility of many organic hole transporting materials such as PVK, TCTA, and CBP [21]. Therefore, balancing hole and electron injection plays an important role on the performance of QD-LEDs. Recently, Peng *et al.* reported a solution-processed multilayer QD-LED with excellent performance and reproducibility by inserting an insulating PMMA layer between the QD layer and the oxide ETL to optimize charge balance in the device [22].

Based on band-gap engineering, doping of ZnO or TiO_2 can tune the conduction band and Fermi level positions, which can enhance the performance of devices [23]–[25]. Among the element-doped ZnO, Mg-doped ZnO ($Mg_xZn_{1-x}O$) attracted a great attention because the Mg 3s orbital hybridize and raise the energy level of the Zn 4s orbital in the ZnO conduction-band minimum (CBM), leading to an increased band gap [26]–[29]. Recently, Hu *et al.* showed a sol-gel method to produce $Mg_xZn_{1-x}O$ layer to improve the open circuit voltage of PbS QD solar cells [30]. Kim *et al.* reported highly efficient inverted QD-LEDs using an Al-doped ZnO (AZO)/Li-doped ZnO (LZO) stacked electron transport layer due to reducing exciton loss at the interface of the ETL and the emissive layer by inserting LZO [31]. To date, among the three primary colors, the development of blue QD-LEDs is lower behind their counterpart of green and red QD-LEDs in terms of device performance [32], [33]. In this study, we demonstrate highly efficient blue QD-LEDs by using a sol-gel method to produce the $Mg_xZn_{1-x}O$ layer as ETL. Compared to inserting an insulting PMMA layer between QDs and ZnO, using a single $Mg_xZn_{1-x}O$ layer can simplify the production process. Mg-doped ratios can adjust the device performance of blue QD-LEDs. The maximum luminescence efficiency of blue QD-LEDs based on the $Mg_{0.10}Zn_{0.90}O$ layer as ETL is improved by approximately two times compared to the control device (ZnO-based QD-LEDs).

2. Experimental Details

ZnO and $Mg_xZn_{1-x}O$ colloidal suspensions were synthesized by hydrolysis and condensation as reported in previous methods [26]. The blue QD-LEDs were fabricated on the ITO-coated glass substrates with a sheet resistance of 15 Ω/□. The substrates were ultrasonically cleaned in detergent, deionized water, acetone, and isopropyl alcohol sequentially for 20 min. Poly (3,4-ethylenedioxythiophene): poly(styrenesulfonate) (PEDOT:PSS) was spin-coated on the precleaned and O_2-plasma-treated ITO substrates at 3000 rpm and it was baked at 120 °C for 30 min to remove residual water and then moved into glove box under the nitrogen-protected environment to perform the subsequent multilayer film processes. Poly (9-vinylcarbazole) (PVK) dissolved in chlorobenzene with 8 mg/mL was spin-coated on the top of PEDOT:PSS at 2000 rpm and dried at 120 °C for 30 min. Blue QD solution from octane with 10 mg/mL was deposited on the top of PVK by spin-coating at 2000 rpm as the emissive layer. It was then heated at 100 °C for 30 min to remove the residual solvent. Then, ZnO or $Mg_xZn_{1-x}O$ solution from ethanol was spin-coated on the top of the emissive layers and then annealed at 80 °C for 30 min. Finally, a 120-nm-thick Al layer was evaporated on top of ZnO or $Mg_xZn_{1-x}O$ as cathode under a vacuum of 4×10^{-4} Pa.

PEDOT: PSS and PVK were purchased from Heraeus and Sigma-Aldrich and used without further purification. Blue ZnCdS/ZnS QDs (Core/shell type) was obtained from Guangdong Poly Optoelectronic Co. Ltd. The testing of device was carried out in the glove box filled with nitrogen at room temperature. The electroluminescent (EL) spectra were recorded by an Ocean Optics fiber optical spectrometer (Maya 2000 Pro). Current-voltage and luminescence-voltage characteristics were measured on a Konica Minolta LS-150 luminance meter with a Keithley 2400 voltage and current source meter. UV-visible absorption spectra of ZnO and $Mg_xZn_{1-x}O$ were recorded with a HP8453A spectrophotometer. The time-resolved PL (TRPL) of the QD films was measured with the Edinburgh Instruments FL 920 Spectrometer at room temperature and under an excitation wavelength of 405 nm. The transmission electron microscopy (TEM) images of ZnO and $Mg_xZn_{1-x}O$ nanoparticles were obtained using JEM-2100HR operated at an accelerating voltage from 100–400 kV. The AFM image and XRD data of the thin films of ZnO and $Mg_xZn_{1-x}O$ were obtained using NT-MDT and Bruker D8 Advance, respectively.

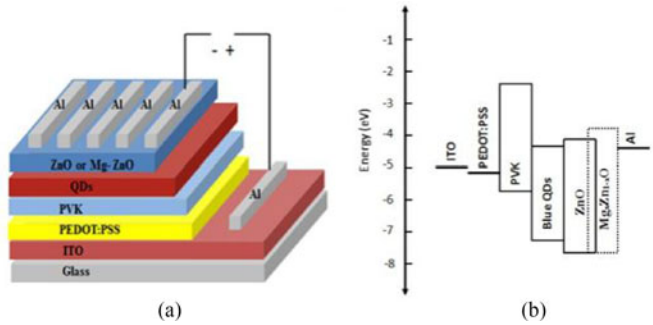

Fig. 1. (a) Structure scheme of QD-LEDs and (b) energy level diagram of the corresponding materials.

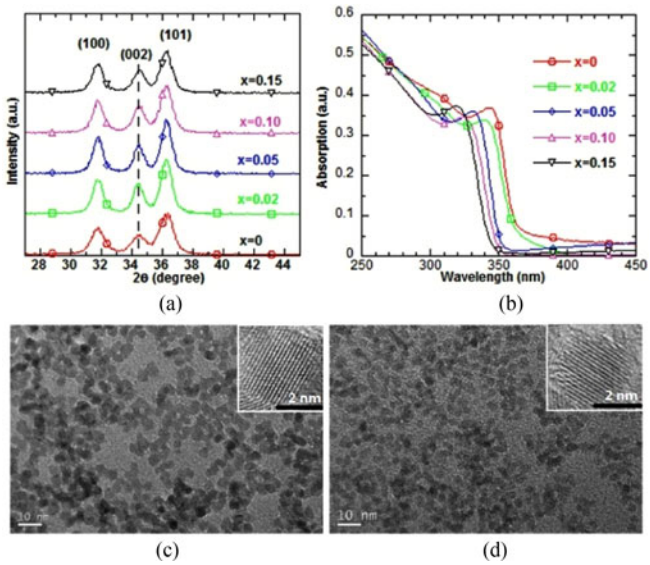

Fig. 2. Characterization of $Mg_xZn_{1-x}O$ films (x = 0, 0.02, 0.05, 0.10, 0.15). (a) XRD patterns, (b) ultraviolet-visible absorption spectra, (c) TEM images of ZnO, and (d) $Mg_{0.10}Zn_{0.90}O$. Representative high resolution TEM image.

3. Results and Discussion

The detailed structure of the QD-LEDs and the energy level diagram of the corresponding materials used in our work are shown in Fig. 1(a) and (b). The highest occupied molecular orbital (HOMO), lowest unoccupied molecular orbital (LUMO), conduction and valence band levels of the materials are taken from the literature [21], [22], [30]. Fig. 2(a) shows the XRD spectra of $Mg_xZn_{1-x}O$ films with different Mg-doped ratios in ZnO. The samples were heated at 80 °C in order to remove the solvent in air and the thickness was about 200 nm. The diffraction peaks at 31.71°, 34.33°, and 36.21° can be indexed to (100), (002), and (101) plane of wurtzite ZnO. No diffraction peaks from MgO or other phases are detected in XRD patterns. The diffraction peaks of (002) gradually migrates to larger diffraction angles when Mg content increases, which is the result of the cationic substitution of Zn^{2+} by the smaller Mg^{2+} leading to reduced crystal lattice parameter. UV-Vis absorption spectra of the corresponding $Mg_xZn_{1-x}O$ films are shown in Fig. 2(b). The absorption edge shifts from 343 nm to 319 nm with Mg concentration increasing from 0% to 15%. This continuous blue-shift is indicative of the widening optical band gap with increasing Mg-doped concentration. The optical band gap is estimated to be the energy at which the absorbance of the absorption edge reached half of its maximum value [34]. The optical band gap of 3.49 eV for ZnO; 3.54 eV for $Mg_{0.02}Zn_{0.98}O$; 3.62 eV for

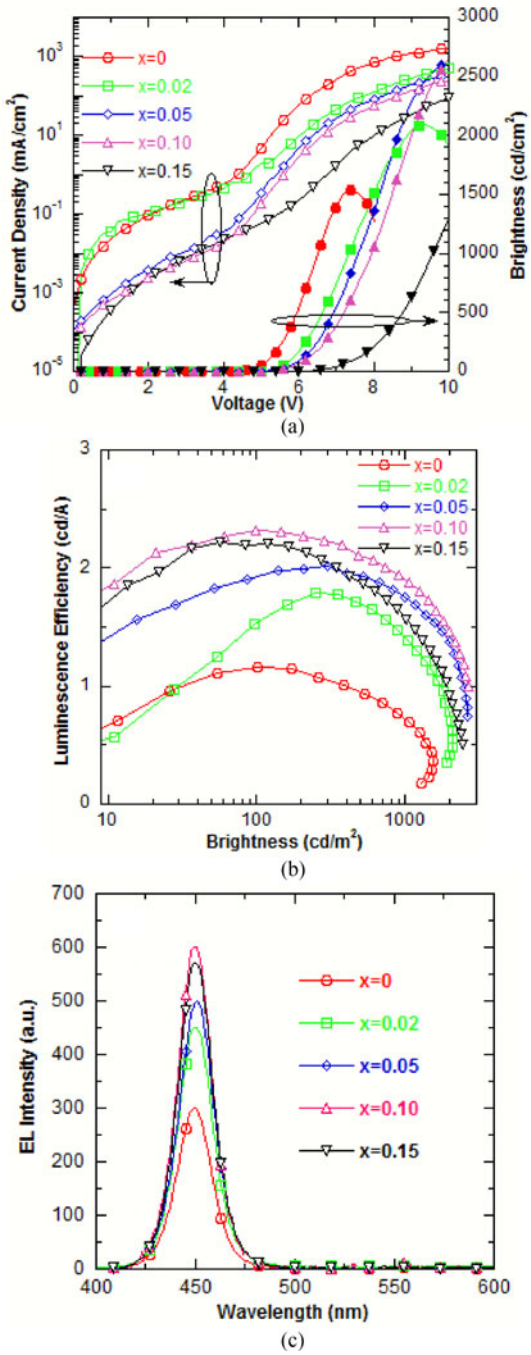

Fig. 3. (a) Current density-voltage-brightness, (b) luminescence efficiency and brightness, and (c) EL emission spectra at 30 mA/cm^2 characteristics of blue QD-LEDs for the different Mg-doped ZnO ratios as ETLs.

$Mg_{0.05}Zn_{0.95}O$; 3.67 eV for $Mg_{0.10}Zn_{0.90}O$; and 3.73 eV for $Mg_{0.15}Zn_{0.85}O$ are obtained, respectively. The size and morphology of ZnO and $Mg_{0.10}Zn_{0.90}O$ nanoparticles were also studied using TEM (Fig. 2(c) and (d)). TEM images show nanocrystals with about spherical shape and average diameter of about 4.06 nm. The average size of $Mg_{0.10}Zn_{0.90}O$ is slightly smaller (~3.97 nm). These results are in agreement with XRD data due to the smaller radii of Mg^{2+} than Zn^{2+}.

TABLE 1
Summarized Device Performances of the Blue QD-LEDs Based on the Different Mg-Doped ZnO Ratios as ETLs

$Mg_xZn_{1-x}O$	V_{on} (V)	B_{max}(cd/cm^2)	LE_{max} (cd/A)
x = 0	4.1	1500	1.1
x = 0.02	4.8	2200	1.8
x = 0.05	4.9	2400	2.0
x = 0.10	5.0	2500	2.3
x = 0.15	6.1	2400	2.2

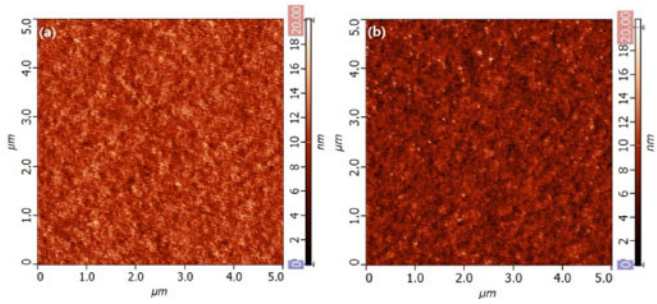

Fig. 4. AFM images of ZnO (a) and $Mg_{0.10}Zn_{0.90}O$ (b) films spin-coated on the top of glass/ITO/PEDOT:PSS/PVK/QDs.

Fig. 3 shows the device characteristics of blue QD-LEDs for different Mg-doped ZnO ratios as ETLs with the same layer thickness. It can be found that the blue QD-LEDs with Mg-doped ZnO as ETLs exhibit a lower current density at the same driving voltage relative to ZnO. This is due to the (CBM) moving upward from 4.05 eV for pure ZnO to 3.64 eV for 15% Mg-doped ZnO [30], thus increasing the electron injection barrier. This can be explained as follows: The valence band minimum (VBM) of ZnO is determined by the O 2p electrons, and the O^{2-} sub-lattice is only slightly modified by the Mg doping, thus keeping the constant VBM position. On the other hand, the CBM of ZnO is dominated by the energy level of Zn 4s state, and when Mg^{2+} cations substitute for the Zn^{2+} sites, the higher energy level of Mg 3s electrons contribute significantly to the CBM, thereby lifting its position [28]–[30]. The luminescence efficiency of the corresponding devices is increased and then reduced with the increasing Mg-doped concentration. The device performance of the different Mg-doped concentration for ZnO as ETLs is summarized in Table 1. The maximum luminescence efficiency of the blue QD-LED increased from 1.1 cd/A for pure ZnO as ETL to 2.3 cd/A for 10% Mg-doped ZnO. Fig. 3(c) shows the EL spectra of the corresponding blue QD-LEDs at 30 mA/cm^2. The EL spectral line shape of the blue QD-LEDs remains almost unchanged for the different Mg-doped concentration. The full width at half maximum (FWHM) is about 21 nm, and the Commission Internationale de l'Enclairage (CIE) coordinates of the corresponding devices are (0.16, 0.03).

We further applied AFM to characterize the film morphology of ZnO and 10% Mg-doped ZnO spin-coated on the top of the glass/ITO/PEDOT:PSS/PVK/QDs (Fig. 4(a) and (b)). All films show smooth surface without voids or cracks. The $Mg_{0.10}Zn_{0.90}O$ film shows a root mean square (RMS) roughness of 1.7 nm lower than ZnO with a RMS of 2.2 nm. Such a smooth surface is beneficial to reduce the leaking current and block the holes.

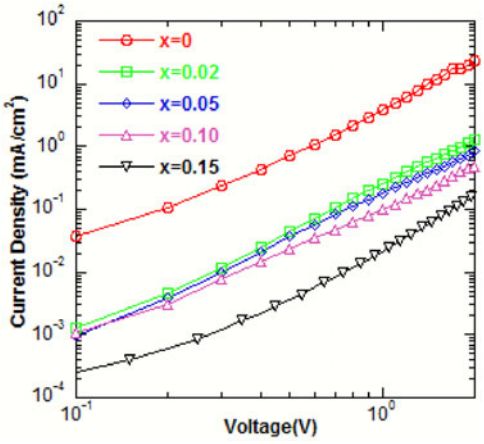

Fig. 5. Current density-voltage curves for the electron-only devices for the different Mg-doped ZnO ratios.

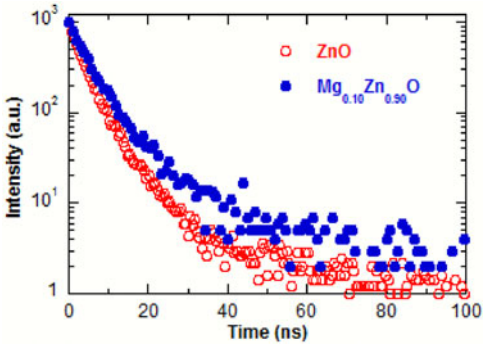

Fig. 6. Time-resolved photoluminance decay for ITO/PEDOT:PSS/PVK/QDs/ZnO or $Mg_{0.10}Zn_{0.90}O$. The thicknesses of the corresponding layers are identical to those blue QD-LEDs.

In order to investigate the Mg-doped ZnO effecting the electron injection in the devices, the electron-only devices were fabricated. Fig. 5 shows the current density-voltage characteristics of the electron-only devices (ITO/Al/$Mg_xZn_{1-x}O$/Al) for the different Mg-doped ZnO concentration. The space-charge-limited-current region ($J \propto V^2$) is demonstrated in Fig. 5. By using Child's law $J = \frac{9u_e\varepsilon_0\varepsilon_r V^2}{8d^3}$, ε_0 , ε_r, u_e, are the vacuum permittivity, relative permittivity, and electron mobility, respectively [22] and d, referring to thickness of films, is 200 nm. By assuming that, the electron mobility of $8.91 \times 10^{-3}\,cm^2/V\,.\,s$ for ZnO, $6.31 \times 10^{-3}\,cm^2/V \cdot s$ for $Mg_{0.02}Zn_{0.98}O$, $2.63 \times 10^{-3}\,cm^2/V \cdot s$ for $Mg_{0.05}Zn_{0.95}O$, $1.78 \times 10^{-3}\,cm^2/V{\cdot}s$ for $Mg_{0.10}Zn_{0.90}O$, and $2.63 \times 10^{-4}\,cm^2/V \cdot s$ for $Mg_{0.15}Zn_{0.85}O$ were obtained, respectively. Obviously, the Mg-doped ZnO can adjust the electron mobility of the $Mg_xZn_{1-x}O$ film at a certain degree. In our device, there is a moderate energetic barrier for hole injection owing to the deep valance band energy level of the blue QDs (Fig. 1(b)). Furthermore, the hole mobility of PVK ($2.5 \times 10^{-6}\,cm^2/V{\cdot}s$) is far lower than the electron mobility of ZnO nanocrystal films ($\sim 10^{-3}\,cm^2/V{\cdot}s$) [21], [22]. This factor can lead to excess electron injection into the QD emissive layer. The Mg-doped ZnO can move upward the conduction band energy level and reduce the electron mobility, in which it is possible to modulate the electron injection from the Al cathodes to the QD emissive layers and eliminate excess electron currents in the blue QD-LEDs by optimizing the Mg-doped concentration in ZnO.

The time-resolved photoluminance (TRPL) decay measurement can further characterize the charge transfer process between ZnO and the QDs. Fitting the TRPL spectra with a bi-exponential equation, the average photoluminance lifetime of the QD films increases from 5.05 ns for ZnO to

6.66 ns for $Mg_{0.10}Zn_{0.90}O$ as ETL (see Fig. 6). The Mg-doped ZnO can modify the blue QDs/ZnO ETL interfacial interaction. These results indicate that the Mg-doped ZnO helps to maintain the charge neutrality of QD emitters and retain their superior emissive properties [22].

4. Conclusions

In summary, we demonstrated a method to adjust the performance of the blue QD-LEDs by a solution-processed Mg-doped ZnO. The introduction of Mg^{2+} ions can move upward the CBM and reduce the electron mobility of ZnO films, resulting in a more balanced hole and electron injection to improve the performance of devices. The maximum luminescence efficiency increases and then reduces with increasing Mg-doped concentration. When the Mg-doped concentration in ZnO increases from 0% to 10%, the maximum brightness and luminescence efficiency increase from 1500 to 2500 cd/cm^2 and from 1.1 to 2.3 cd/A, respectively. Therefore, the Mg-doped ZnO can be used as effective ETLs for QD-LEDs.

References

[1] S. Kim *et al.*, "Near-infrared fluorescent type II quantum dots for sentinel lymph node mapping," *Nature Biotechnol.*, vol. 22, pp. 93–97, 2004.

[2] Y. Zhang, Y. Li, and X. P. Yan, "Aqueous layer-by-layer epitaxy of type-II CdTe/CdSe quantum dots with near-infrared fluorescence for bioimaging applications," *Small*, vol. 5, pp. 185–189, 2009.

[3] C. Steinhagen, M. G. Panthani, V. Akhavan, B. Goodfellow, B. Koo, and B. A. Korgel, "Synthesis of Cu_2ZnSnS_4 nanocrystals for use in low-cost photovoltaics," *J. Amer. Chem. Soc.*, vol. 131, pp. 12554–12555, 2009.

[4] W. L. Ma, J. M. Luther, H. M. Zheng, Y. Wu, and A. P. Alivisatos, "Photovoltaic devices employing ternary Pbs_XSe_{1-X} nanocrystals," *Nano Lett.*, vol. 9, pp. 1699–1703, 2009.

[5] J. H. Bang and P. V. Kamat, "Quantum dot sensitized solar cells. A tale of two semiconductor nanocrystals: CdSe and CdTe," *ACS Nano*, vol. 3, pp. 1467–1476, 2009.

[6] M. Nam, S. Kim, M. Kang, S. Kim, and K. Lee, "Efficiency enhancement in organic solar cells by configuring hybrid interfaces with narrow bandgap PbSSe nanocrystals," *Organic Electron.*, vol. 13, pp. 1546–1552, 2012.

[7] Y. Shirasaki, G. J. Supran, M. G. Bawendi, and V. Bulović, "Emergence of colloidal quantum-dot light-emitting technologies," *Nature Photon.*, vol. 7, pp. 13–23, 2012.

[8] P. Prabhakaran, W. J. Kim, K.-S. Lee, and P. N. Prasad, "Quantum dots (QDs) for photonic applications," *Opt. Mater. Exp.*, vol. 2, pp. 578–593, 2012.

[9] T.-H. Kim *et al.*, "Full-colour quantum dot displays fabricated by transfer printing," *Nature Photon.*, vol. 5, pp. 176–182, 2011.

[10] X. Yang *et al.*, "Solution processed tungsten oxide interfacial layer for efficient hole-injection in quantum dot light-emitting diodes," *Small*, vol. 10, pp. 247–252, 2014.

[11] J. Kwak, J. Lim, M. Park, S. Lee, K. Char, and C. Lee, "High-power genuine ultraviolet light-emitting diodes based on colloidal nanocrystal quantum dots," *Nano Lett.*, vol. 15, pp. 3793–3799, 2015.

[12] J. Kwak *et al.*, "Bright and efficient full-color colloidal quantum dot light-emitting diodes using an inverted device structure," *Nano Lett.*, vol. 12, pp. 2362–2366, 2012.

[13] G. Cheng, M. Mazzeo, S. Carallo, H. Wang, Y. Ma, and G. Gigli, "Full spin-coated multilayer structure hybrid light-emitting devices," *Appl. Phys. Lett.*, vol. 97, 2010, Art. no. 103107.

[14] A. Castan, H.-M. Kim, and J. Jang, "All-solution-processed inverted quantum-dot light-emitting diodes," *ACS Appl. Mater. Interfaces*, vol. 6, pp. 2508–2515, 2014.

[15] W. K. Bae *et al.*, "Multicolored light-emitting diodes based on all-quantum-dot multilayer films using layer-by-layer assembly method," *Nano Lett.*, vol. 10, pp. 2368–2373, 2010.

[16] Q. Sun *et al.*, "Bright, multicoloured light-emitting diodes based on quantum dots," *Nature Photon.*, vol. 1, pp. 717–722, 2007.

[17] W. K. Bae, J. Kwak, J. W. Park, K. Char, C. Lee, and S. Lee, "Highly efficient green-light-emitting diodes based on CdSe@ZnS quantum dots with a chemical-composition gradient," *Adv. Mater.*, vol. 21, pp. 1690–1694, 2009.

[18] L. Qian, Y. Zheng, J. Xue, and P. H. Holloway, "Stable and efficient quantum-dot light-emitting diodes based on solution-processed multilayer structures," *Nature Photon.*, vol. 5, pp. 543–548, 2011.

[19] W. Xu *et al.*, "Efficient inverted quantum-dot light-emitting devices with TiO_2/ZnO bilayer as the electron contact layer," *Opt. Lett.*, vol. 39, pp. 426–429, 2014.

[20] C.-Y. Huang and J.-H. Lai, "Efficient polymer light-emitting diodes with ZnO nanoparticles and interpretation of observed sub-bandgap turn-on phenomenon," *Organic Electron.*, vol. 32, pp. 244–249, 2016.

[21] M. D. Ho, D. Kim, N. Kim, S. M. Cho, and H. Chae, "Polymer and small molecule mixture for organic hole transport layers in quantum dot light-emitting diodes," *ACS Appl. Mater. Interfaces*, vol. 5, pp. 12369–12374, 2013.

[22] X. Dai *et al.*, "Solution-processed, high-performance light-emitting diodes based on quantum dots," *Nature*, vol. 515, pp. 96–99, 2014.

[23] I. Y. Kim *et al.*, "Comparative study of quaternary Mg and Group III element co-doped ZnO thin films with transparent conductive characteristics," *Thin Solid Films*, vol. 570, pp. 321–325, 2014.

[24] S. W. Shin *et al.*, "Development of transparent conductive Mg and Ga co-doped ZnO thin films: Effect of Mg concentration," *Surf. Coating Technol.*, vol. 231, pp. 364–369, 2013.
[25] J. Yang, H. Zhang, X. Wang, L. Miao, and Y. Yang, "Optical properties of Ag doped ZnO nanocrystals prepared by hydrothermal and photodeposition method," *J. Mater. Sci., Mater. Electron.*, vol. 24, pp. 3430–3434, 2013.
[26] E. B. Manaia, R. C. K. Kaminski, B. L. Caetano, V. Briois, L. A. Chiavacci, and C. Bourgaux, "Surface modified Mg-doped ZnO QDs for biological imaging," *Eur. J. Nanomed.*, vol. 7, pp. 109–120, 2015.
[27] X. Li, Y. Liu, J. Song, J. Xu, and H. Zeng, "MgZnO nanocrystals: Mechanism for dopant-stimulated self-assembly," *Small*, vol. 11, pp. 5097–5104, 2015.
[28] S. Sharma *et al.*, "Highly efficient green light harvesting from Mg doped ZnO nanoparticles: Structural and optical studies," *J. Alloys Compounds*, vol. 552, pp. 208–212, 2013.
[29] L.-N. Bai, J.-S. Lian, and Q. Jiang, "Optical and electronic properties of wurtzite structure $Zn_{1-x}Mg_xO$ alloys," *Chin. Phys. Lett.*, vol. 28, 2011, Art. no. 117101.
[30] L. Hu *et al.*, "Graphene doping improved device performance of ZnMgO/PbS colloidal quantum dot photovoltaics," *Adv. Funct. Mater.*, vol. 26, pp. 1899–1907, 2016.
[31] H. M. Kim, D. Geng, J. Kim, E. Hwang, and J. Jang, "Metal-oxide stacked electron transport layer for highly efficient inverted quantum-dot light emitting diodes," *ACS Appl. Mater. Interfaces*, vol. 8, pp. 28727–28736, 2016.
[32] P. O. Anikeeva, J. E. Halpert, M. G. Bawendi, and V. Bulović, "Quantum dot light-emitting devices with electroluminescence tunable over the entire visible spectrum," *Nano Lett.*, vol. 9, pp. 2532–2536, 2009.
[33] W. Y. Ji *et al.*, "High color purity ZnSe/ZnS core/shell quantum dot based blue light emitting diodes with an inverted device structure," *Appl. Phys. Lett.*, vol. 103, 2013, Art. no. 053106.
[34] E. A. Meulenkamp, "Synthesis and growth of ZnO nanoparticles," *J. Phys. Chem. B.*, vol. 102, pp. 5566–5572, 1998.